Research Square

Preprints are preliminary reports that have not undergone peer review.
They should not be considered conclusive, used to inform clinical practice,
or referenced by the media as validated information.

Programmed cell death and redox metabolism protect Chlamydomonas reinhardtii populations from the galactic cosmic environment on the Artemis-1 mission

Timothy G. Hammond

hammondoutofoffice@yahoo.com

Durham VA Health Care System

Sajanlal Panikkanvalappil

Harvard Medical School

Patricia L. Allen

Durham VA Health Care System

Hamid Kian Gaikani

The University of British Columbia

Corey Nislow

The University of British Columbia

Guri Giaever

The University of British Columbia

Ye Zhang

NASA-Kennedy Space Center, Utilization & Life Sciences Office

Howard G. Levine

NASA-Kennedy Space Center, Utilization & Life Sciences Office

Ramona Gaza

Leidos

Dinah Dimapilis

NASA Johnson Space Center

Howard W. Wells

The Bionetics Corporation

James M. Russick

The Bionetics Corporation

Pierre M. Durand

University of the Witwatersrand

Holly H. Birdsall

Baylor College of Medicine

Article

Keywords: cosmic radiation, Chlamydomonas reinhardtii, protection, β-carotene, Dsup, tardigrade, spaceflight, redox, Artemis-1

Posted Date: November 11th, 2024

DOI: https://doi.org/10.21203/rs.3.rs-5268750/v1

License: This work is licensed under a Creative Commons Attribution 4.0 International License.
Read Full License

Additional Declarations: No competing interests reported.

Version of Record: A version of this preprint was published at Scientific Reports on July 2nd, 2025. See the published version at https://doi.org/10.1038/s41598-025-05419-w.

Abstract

We hypothesized that on the Artemis I mission, exposure to the galactic cosmic environment, specifically microgravity, lack of convection, and galactic cosmic radiation, would reduce survival of *Chlamydomonas reinhardtii*, a green unicellular flagellate alga, through the process of necrosis. An alternative hypothesis was that the radiation stimulus would induce a population survival response via a programmed cell death pathway.

The *Chlamydomonas* strains were spotted on nutrient agar acetate plates and flown on Artemis I in the new Moonshot hardware that provided six hours of light daily to synchronize the algal cell cycle and tracked temperature, power use, and gravity over time. Synchronous ground controls were run in parallel. Analysis included spectrophotometry of chlorophylls and photosystems, flow cytometry of cell viability and lipid content, and Raman spectroscopy to identify DNA damage and cellular proteins. To test for radiation protection, select strains carried the tardigrade damage suppressor (*Dsup*) gene known to protect animal cells against gamma and ionizing radiation, dehydration, and temperature extremes in ground-based studies.

A new flight hardware termed “Moonshot” was designed, built, and flown. “Moonshot” performed flawlessly, and is now available as flight-certified, flight-proven hardware for timed illumination and monitoring for flight and terrestrial applications.

Within the limitations of the physical handling of specimens necessitated by the Artemis-1 mission flight around the Moon with exposure to the galactic cosmic environment:

1. Flown samples exposed to cosmic radiation were more viable than ground controls, with increased programmed cell death and decreased necrosis.

2. There was no difference in *Chlamydomonas* growth or content of chlorophylls and photosystems in flown versus ground controls, ruling out energy metabolism as the mediator of cell death.

3. Raman spectroscopy analysis showed that the redox-protective protein beta-carotene, a known cell death mediator, was increased during flight around the moon.

4. Compared to control inserts, insertion of the *Dsup* tardigrade gene was protective both on the ground and in flight.

Introduction

The study of the biological effects of the galactic cosmic environment has a dual purpose. First, understanding the biology of galactic cosmic environment should guide development of protective measures for astronauts flying beyond low Earth orbit [1], as well as leveraging biological systems to produce meaningful biologics in the space environment [2, 3]. The second purpose is to begin to explore whether galactic cosmic environment mimics have utility for ground-based clinical applications [4].

Experiments flown on the Artemis 1 mission that circumnavigated the Moon, represent the first opportunity since the Apollo era to return to Earth biological samples exposed to the galactic cosmic environment (https://www.nasa.gov/reference/artemis-i/). To understand the novelty of this opportunity, it is critical to remember that the International Space Station (ISS) is inside the radioprotective Van Allen Belts. Although experiments and personnel on the ISS are exposed to microgravity, reduced convection, and more radiation than on Earth [5], they are shielded from the vast majority of galactic cosmic radiation by the van Allen Belts [6].

The green alga *Chlamydomonas reinhardtii* was selected as the biological model system. It is a well-characterized, motile, single-celled green alga whose genome is fully sequenced and is relatively easy to engineer molecularly. During previous growth in space, a light-dependent increase in photosystem II has been observed [7].

The primary hypothesis was that exposure to galactic cosmic environment would reduce *Chlamydomonas* survival through unregulated cell death mechanisms called necrosis. An alternative balancing argument was that the radiation stimulus would induce a population survival response via a programmed cell death (PCD). PCD is sometimes a population survival mechanism in microalgae [8–10].

Measurements on the galactic cosmic environment exposed *Chlamydomonas*, and ground-based controls, included metabolic parameters of energy metabolism, mechanisms of cell death, and production of natural products.

Raman spectroscopy was used for real-time chemical analysis of the *Chlamydomonas* cells [11, 12]. The Curiosity rover on Mars uses fluorescence and Raman spectroscopy to search for organic molecules as a possible sign of life [13], but the potential of the biological application of these techniques is only starting to be realized [11, 12]. Raman spectroscopy is a non-destructive and non-invasive technique, which offers several advantages in studying various stress-induced (including radiation) biomolecular modifications at the single-cell level without altering their integrity [14, 15]. Moreover, the sensitivity of Raman spectroscopy enables the detection of subtle changes in cellular redox metabolism, which is fundamental in elucidating the dynamic alterations in the levels of redox-active species, as well as the cellular response to oxidative stress caused by cosmic radiation.

Further, several lines of evidence show that multiple tardigrade genes, including *Dsup*, afford protection from a diverse array of stresses including various forms of radiation present in low Earth orbit [16, 17]. An aliquot of the green algae strains flown in this experiment had the tardigrade gene *Dsup* inserted into the cell nucleus to test for protection from the galactic cosmic environment.

The initiative began with the design and fabrication of affordable new flight hardware (named Moonshot) to support the growth of *Chlamydomonas reinhardtii* [18], while simultaneously meeting the constraints of the Artemis I mission profile (https://www.nasa.gov/mission/artemis-i/).

Discussion

Artemis-1

The effects of the galactic cosmic environment on biological samples remains largely unknown, as the samples returned on Artemis-1 were the first samples returned following exposure to galactic cosmic environment beyond low Earth orbit since the Apollo era.

Viability shift: protection from cosmic radiation

The major finding of this study is that our hypothesis that exposure to the galactic cosmic environment would reduce *Chlamydomonas* survival through the process of necrosis was disproven. The alternative balancing argument that the radiation stimulus would induce a population survival response via a PCD pathway is supported. These findings are initially surprising, as the galactic cosmic environment contains high linear energy transfer (LET) particles that evoke complex DNA and other cellular damage [19, 20], including significant damage to biological organisms, that include space radiation-induced carcinogenesis, cardiovascular disease, and central nervous system deficiencies [21, 22]. Approximately 70% of galactic cosmic particles are high energy protons with similar relative biological effectiveness (RBE) slightly higher than low LET radiation such as gamma rays and X-rays. Protons are passing through living organisms with uniform distributions. However, heavier particles, which can cause devastating consequences on cells with direct hits, are distributed non-uniformly through the cell populations. Secondary effects are then caused by secondary particles or by signal transduced from the cells with direct hits [26, 27, 28, 29].

The findings can be explained by understanding the properties of PCD [8, 9, 23, 24]. PCD is a population stress response that is both adaptive and plastic [9]. Initial population decline due to PCD in response to stress helps the population rebound [9]. PCD can be a group-level stress response, where there is reconstitution of population density by expansion of survivors [23]. Microgravity simulation has been found to induce PCD in multiple cells, and tissues, both *in vivo* and *in vitro* [19].

In *Chlamydomonas reinhardtii*, PCD provides differential species-specific fitness effects that not only benefit others of the same species, but also have an inhibitory effect on the growth of other species [8]. The phenomenon of programmed cell death benefiting relatives is not limited to *Chlamydomonas* as it is also true in the green microalga *Ankistrodesmus*, (Sphaeropleales, Selenastraceae) [25].

There are many methods to assay PCD in algae and specifically in, *Chlamydomonas reinhardtii* [10]. PCD and necrosis assayed by flow cytometry analysis of Annexin V binding and propidium iodide uptake (described as a ‘hard sign’ of PCD), or cell size, give the best specificity and sensitivity of methods available within the parameters of the Artemis-1 mission profile [26]. Multiparameter flow cytometry can provide more robust data analysis [27], but no matter which combination of parameters we compared,

there was always more overall cell survival, more PCD, and less necrosis in the spaceflight samples compared to the ground controls.

Insertion of the tardigrade gene Dsup: **Protection from cosmic radiation**

Tardigrades are microscopic animals renowned for their ability to survive a vast array of environmental extremes, including essentially complete desiccation for up to a decade as well as severe radiation damage [28–31]. Tardigrades survived ten days in the temperature, vacuum, and unshielded cosmic radiation of space aboard European Space Agency's FOTON-M3 mission [31]. Several mechanisms contribute to the tardigrades' radio-resistance, and Tardigrade Disordered Proteins (TDPs) provide remarkable resistance to these stresses. RNA-seq and differential gene expression analysis revealed 11 TDP genes that are induced up to 20-fold during desiccation, along with a related class of TDPs that are expressed constitutively at extremely high levels. Amongst the tardigrade intrinsically disordered proteins (*Dsup*; Cytoplasmic, Secreted, and Mitochondrial Abundant Heat Soluble protein; and late embryogenesis-abundant proteins (LEA)) [32], *Dsup* was our choice to insert into the nucleus of *Chlamydomonas* based on evidence that *Dsup* suppresses the occurrence of DNA breaks by radiation in human-cultured cells[17]. As tardigrades have high resistance to diverse stress factors associated with cosmic journeys, they are the focus of intense study by astrobiologists [33, 34].

Inserting *Dsup* into the nucleus of *Chlamydomonas* did indeed improve survival, both in space and in the ground-based control samples. The substantial increase in survival of *Chlamydomonas* in space determined that the starting baseline survival of the two groups were very different. Certainly, *Dsup* induced a smaller increase in survival in space than on the ground, but it is unclear whether this is a ceiling phenomenon as the *Dsup*-induced final survival level is no different in the flight and ground groups.

Raman spectroscopy and redox metabolism during spaceflight

Redox signaling is activated in diverse tissues and cell systems by varied forms of stress, including radiation, spaceflight, and simulated microgravity [35, 36]. Stress-induced redox activation can be alternatively adaptive or contribute to pathological outcomes [36]. Targeting of redox metabolism has been proposed for mitigation of radiation injury [37]. Carotenoids are a class of pigments critical for photoprotection [38]. It is likely that cosmic ray and/or microgravity induced stress in *Chlamydomonas* could potentially activate their defense mechanisms to prevent the radiation damage, which can result in enhanced carotenoid biosynthesis and production of carotenoids [39]. β-carotene administration is the subject of multiple clinical trials aiming to decrease cardiovascular disease or cancer risk [40].

The differential activation of unique survival strategies under space conditions, as observed through Raman spectroscopy in *Chlamydomonas*, highlights the complex nature of cellular responses to environmental stresses such as radiation and microgravity. The Raman spectroscopic analyses detected two types of cells, which we have designated as Type I and Type II. The enhanced production of

carotenoids seen in Type II cells from the flown sample served as a protective mechanism, likely activated to scavenge reactive oxygen species generated by stress, thereby mitigating potential radiation damage. This aligns with various studies suggesting that carotenoid biosynthesis can be stimulated as an adaptive response to environmental challenges [41, 42]. We also saw some algal cells without/weak β-carotene Raman bands (Type I) in the same flight samples, which is consistent with the flow cytometry and fluorescence microscopy data presented in this manuscript, that not all the cells can survive the cosmic ray stress.

The lack of significant carotenoid vibrations in Type I cells (also in the azide-killed samples) suggests that these cells may not effectively induce protective responses, making them more susceptible to radiation-induced damage. This observation is critical as it implies that not all cells within a population will uniformly respond to stress, highlighting the importance of understanding individual cellular adaptations in space biology. In addition, our findings also underline the utility of Raman spectroscopy in detecting subtle changes in cellular composition and stress responses, such as shifts in carotenoid ratios and alterations in the electronic environment around chlorophyll molecules. These insights are pivotal for developing strategies to enhance the resilience of microorganisms in space.

Chlorophylls and photosystems

There was no detectible change in chlorophylls and photosystems during the flight, excluding energy metabolism as the cause of the changes in programmed cell death observed.

Cost and practicality of Moonshot hardware

Advances in materials, microelectronics, and molecular and cellular biology technologies provided a firm basis to produce cost-effective customized spaceflight hardware. Bionetics Corporation’s engineering team developed new hardware, called moonshot, within a cost that could be supported from the funded grant. Moonshot holds three 10 cm segmented Petri dishes, and provides timed daily blue and red-light sample exposure, while recording state, battery voltage, temperature, and acceleration in 3 dimensions at programmable times. The Moonshot hardware performed flawlessly, providing flight certified, flight proven hardware for future biological investigations [18].

Radiation dose

The two sensors adjacent to the Moonshot hardware on Artemis I had different radiation spectrum sensitivities. Artemis I was initially planned in 2018, and at that time crew active dosimeters (CADs) were selected for radiation detection. When radiation area monitors (RAMs) became available in 2020, they were added to the radiation monitoring profile in flight [6]. The RAM is designed to record radiation exposure at a specific location, while a CAD is designed to move with a crew member. In our case both dosimeters were static on the hardware. The CAD was expected to have a slightly higher reading, due to

differences in radiation spectrum collection by the two dosimeters. Solar energetic particles from solar flares or sunspots can moderate the observed radiation levels but no solar flares or sunspots occurred during the Artemis I mission. Other radiation detectors flown on the Orion capsule on the Artemis I mission included six CADS distributed around the capsule, and the Hybrid Electronic Radiation Assessor (HERA) system. HERA is a Timepix-based ionizing radiation detector built for NASA Exploration-class crewed missions [43]. Two 'phantoms' of the Matroshka AstroRad Radiation Experiment (MARE) flew in two of passenger seats (Seat #3 and Seat #4) in the Orion capsule [44].

The levels of radiation recorded in the RAM and CAD detectors during the Artemis-1 flight are similar to levels seen during the Curiosity rover flight to Mars, if the same period of time is extracted from the total radiation levels reported [45]. The radiation levels during the Artemis-1 mission flight were far greater than ambient terrestrial levels [46], about three times the levels on the ISS [5], and about the same total exposure as a medical computed tomography (CT) abdominal scan with and without contrast (Table 1) [47]. CAD and RAM measure quantity, but do not define the spectrum of the linear energy transfer for the galactic cosmic environment [6]. The radiation risk is directly influenced by this spectrum as the quality of the radiation characterized by its pattern of energy deposition at the micron/DNA scale determines damage [20]. The linear energy transfer profile as the Curiosity rover flew to Mars has been documented [45]. The linear energy transfer spectrum for the Artemis-1 flight has been defined [48], but a basis for biological interpretation is lacking.

Parsing the elements of the galactic cosmic environment

Ideally, we would model and study the elements of microgravity, convection, and radiation of the galactic cosmic environment individually in ground-based studies. Unfortunately, the technical expertise to parse the elements of the galactic cosmic environment are lacking. Microgravity simulations balance gravity with an induced equal and opposite force, typically using liquid culture environment [49]. These model systems introduce multiple new stimuli, limiting comparison to an element of the galactic cosmic environment. There are scant, if any, mechanisms to model biological responses to low convection [49]. NASA's ground-based Galactic Cosmic Ray Simulator at the NASA Space Radiation Lab [4] will be critical to understand the biology of galactic cosmic radiation but is beyond the scope and resources of the current study.

Benefits and limitations

The galactic cosmic environment poses many challenges but also provides opportunities. For life to survive in cosmic radiation, the first steps begin with research to understand the fundamental effect on biological processes; understand the fundamental biology of life during exposure to cosmic radiation; contribute knowledge to reduce human health risk beyond low Earth orbit; and contribute to improved system performance and reduced system risk. This data set is a first step to answer fundamental

questions such as can we survive and thrive beyond Earth, and can we use knowledge gained from studying the biological effects of galactic space radiation for Earth-based benefits?

Conclusions

Within the limitations of the physical handling of specimens necessitated by the Artemis-1 mission, flight around the Moon with galactic cosmic environment exposure allows multiple conclusions. Flown samples exposed to the galactic cosmic environment were more viable than ground controls with increased programmed cell death and decreased necrosis. There was no difference in *Chlamydomonas* growth or content of chlorophylls and photosystems in flown versus ground controls, ruling out energy metabolism as the mediator of cell death. Compared to control inserts, insertion of the *Dsup* tardigrade gene was protective both on the ground and in flight, although the ground effect was far larger numerically. Raman spectroscopy analysis showed that the redox-protective protein beta-carotene, a known cell death mediator, was increased during flight around the Moon, defining this technology as an important new non-destructive tool for analysis of biological space flight samples. An inexpensive simple new flight hardware, termed Moonshot, can perform flawlessly, and is available as flight-certified, flight-proven hardware for timed illumination and monitoring of samples for flight and terrestrial applications.

Methods and materials

Chlamydomonas reinhardtii

Chlamydomonas reinhardtii (CC-125 wild type mt+ [137c]), were purchased from the University of Minnesota *Chlamydomonas* collection (Minneapolis, MN).

The *Chlamydomonas* were spotted on Tris-acetate-phosphate (TAP) agar plates, and aliquots reseeded onto fresh plates robotically every 2 weeks. TAP was 20 ml 1M Tris base, 1 ml phosphate K_2HPO_4/KH_2PO_4 buffer, 1 ml Hunter's trace metals, 10 ml of solution A [NH_4Cl, $MgSP_4.7H_2O$, 1 ml $CaCl_2.2H_2O$], glacial acetic acid pH 7 made up to 1 liter with distilled water.

Chemicals

Life Technologies was the vendor for Annexin V, Alexa Fluor 488 conjugate, and Annexin-binding buffer – "5X concentrate" for flow cytometry. All other chemicals were purchased from Sigma/Aldrich, now Millipore-Sigma (Burlington, MA). Hutner's trace elements were purchased from the University of Minnesota (Minneapolis, MN).

Equipment

Spectrophotometry was performed on a Molecular Dynamics (San Jose CA) M5e Spectrophotometer. Flow cytometry was performed on a Becton-Dickinson Accuri C + Plus flow cytometer (Franklin Lakes, NJ). Raman spectra were collected using a Renishaw inVia Raman Microscope coupled with Leica

DM2500M microscope at the Dana-Farber Cancer Institute/Harvard Med. School, Boston, MA. A 785 nm diode laser was used for the surface enhanced Raman spectroscopy measurements.

Moonshot hardware was designed and built by The Bionetics Corporation, (Kennedy Space Center, Brevard County, FL) as an ultralow-power growth system for use on Artemis-1 [18]. Each of the three growth modules holds one standard 100 mm diameter circular Petri dish. The plates are illuminated with blue (~450 nm) and red (~660 nm) light-emitting diode (LED) lights continuously for 6 h in every 24 h. The combination of red and blue light is optimum for *Chlamydomonas* [50, 51]. The hardware monitors and records the temperature of the experiment, the power level, and draw from the batteries (as an indication that the lights were turned on and off), as well as the acceleration levels in three axes.

Once activated and loaded with the biological samples, the flight hardware was placed in a custom lathed form-fitting Styrofoam support and encased in a Nitex bag. The assembly was termed the BioExpt-01 Science Bag.

Crew Active Dosimeter (CAD) and Radiation Area Monitor (RAM) radiation detectors were placed adjacent to the biological flight hardware in the BioExpt-01 Science Bag. The detectors had been assembled and delivered to NASA/Kennedy Space Center prior to flight by the Space Radiation Analysis Group based at NASA Johnson Space Center (JSC) by Human Health and Performance Directorate/Leidos personnel. The detectors were collected post-flight and data was analyzed at NASA JSC [6].

Artemis-1 flight

After an initial delay of 19 days on the launch pad, the Artemis − 1 mission was launched from Kennedy Space Center (KSC) on November 16, 2022 for a planned 25-day space mission. Orion completed one flyby of the Moon on November 21, followed by a distant retrograde orbit for six days and then a second flyby of the Moon on November 25, and subsequently returned to Earth. The Orion capsule was recovered from the Pacific Ocean, returned to California, and transported back to KSC by truck. However, the Space Biology experiments were first removed from Orion in California, flown on an accompanied commercial flight to Kennedy Space Center at ambient temperature (without security radiation scanning) and the Moonshot hardware containing the samples, released to the investigators 9 days after the landing. The sample arrived back in the investigator's lab three days later, after decommissioning of the hardware at Bionetics facility adjacent to KSC. The samples for the payload described in the report were in the hardware for a total of 56.5 days (Fig. 1). The flight samples were exposed to microgravity in space, but also gravity transitions during launch and re-entry.

Analysis

Spectrophotometry

Chlamydomonas colonies were scraped from the agar, washed three times in phosphate buffered saline, resuspended in TAP buffer and assayed by spectrophotometry for chlorophyll a (absorbance at 436 nm), chlorophyll b (absorbance at 472 nm), photosystem I and II (absorbance at 700 nm and 680nm respectively but the peaks are too broad to separate), cytochrome f (absorbance at 554 nm), and protein content (absorption at 800 nm). Net absorbance for each wavelength was calculated by subtracting the background absorbance of TAP buffer alone. The net absorbance values were then normalized to the protein content as measured by absorbance at 800 nm.

Flow Cytometry

Six colonies from flight and ground plates, plus four *Dsup* colonies from flight and ground plates, were harvested and resuspended in annexin-binding buffer, which is a phosphate buffer with calcium. The aggregates were disrupted by vortexing and then filtered through a 70µm nylon mesh to remove clumps that would plug the flow cytometer. The resuspended *Chlamydomonas* samples were aliquoted 100 µl per well into V-bottom microtiter plates. Individual aliquots were either stained with Alexa Fluor 488-annexin (5 µl/well) and propidium iodide (PI) (1 µl) to identify PCD and necrosis, or Nile Red (1:100 dilution from a stock solution of 100 µg ml^{-1} in methanol) with 0.005% Triton-X (1:100 dilution from a stock solution of 0.5% in water) permeabilization to measure lipid content.

We counted 2,000 *Chlamydomonas* cells from each sample. Background signal was estimated by appropriate no-dye controls. In every flow cytometry run, quality controls were performed on the instrument with three-color fluorescent beads, followed by assay of five control tubes: (1) no dyes, (2) Alexa fluor 488 annexin binding alone, (3) propidium iodide alone, (4) Alexa fluor 488 annexin binding with propidium iodide, and (5) Nile Red alone.

Flow cytometric and spectrophotometric data were evaluated by two-tailed Student's t-test comparing heat- or cold-exposed *Chlamydomonas* to the relevant room temperature control.

Single-cell confocal Raman spectroscopy of Chlamydomonas reinhardtii

Multiple colonies of *Chlamydomonas* were harvested from a ground plate, and flight plate. The samples included colonies flown live and colonies pretreated with azide before flight. The colonies were harvested into 1.5 ml Eppendorf tubes with 500 µL TAP and resuspended by pipetting and vortexing. The resultant *Chlamydomonas* solution was filtered through a 70 µm mesh into 12 x 74 mm polypropylene tubes to remove multicellular aggregates. The remaining solution of cells was divided into two 500 µL Eppendorf tubes, spun at 3000g for 1 minute to pellet the cells, and the supernatant aspirated. One tube was left to air dry. The second tube had 100 µL of 10% electron microscopy paraformaldehyde added, incubated for 10 min, and then was spun to pellet the cells before the supernatant was aspirated. This paraformaldehyde-fixed sample was washed with 500 µL deionized water, spun, and the supernatant aspirated.

A 2 µl aliquot of each sample rehydrated with distilled water was spotted on a quartz slide (25 mm x 25 mm x 1 mm) that was kept on a microscopic glass slide covered with aluminum foil. This substrate

showed minimal background signal compared to various other substrates we tried such as glass, CaF_2 and Al_2O_3. A silicon wafer was not used as it has a strong Raman band at 521 cm^{-1} and interfered with the current analysis. The samples were air dried at room temperature and were analyzed. A Horiba LabRAM Odyssey Raman microscope was used for the Raman spectral characterization of these samples. Laser power density was optimized in order to achieve better spectral intensity with characteristic Raman bands, which were not present at lower laser power densities. Exposure time and laser intensity were optimized by conducting a series of experiments to prevent charring of the samples to eliminate any unwanted signals due to laser-induced biomolecule denaturation. A 785 nm laser was used to acquire Raman spectra (acquisition time of 30 s with 300 lines/mm grating). First, white light focused on the individual algal cells at a magnification of 100X. Then, Raman spectra were collected in the range of 400–1800 cm^{-1}. The spectral baselines were pre-processed by polynomial fitting.

Statistics

Flow cytometric and spectrophotometric data are presented as geometric mean ± standard error with six replicates (unless otherwise noted). Correlations were analyzed by Statistica 6.1 (StatSoft Inc. Tulsa OK) using correlation matrix product moment and partial correlations.

For the Raman spectral analysis: Spectra were collected from five or more algal samples across three different colonies exposed to various conditions and subsequently averaged to better represent statistical variations in the intensities of vibrations corresponding to various biomolecular components within the spectra. The standard deviation of these intensities under different conditions was illustrated using error bars in the histogram to provide a clear visualization of the variability and reliability of our measurements.

Methods and materials

Chlamydomonas reinhardtii

Chlamydomonas reinhardtii (CC-125 wild type mt+ [137c]), were purchased from the University of Minnesota *Chlamydomonas* collection (Minneapolis, MN).

The *Chlamydomonas* were spotted on Tris-acetate-phosphate (TAP) agar plates, and aliquots reseeded onto fresh plates robotically every 2 weeks. TAP was 20 ml 1M Tris base, 1 ml phosphate K_2HPO_4/KH_2PO_4 buffer, 1 ml Hunter's trace metals, 10 ml of solution A [NH_4Cl, $MgSP_4.7H_2O$, 1 ml $CaCl_2.2H_2O$], glacial acetic acid pH 7 made up to 1 liter with distilled water.

Chemicals

Life Technologies was the vendor for Annexin V, Alexa Fluor 488 conjugate, and Annexin-binding buffer – "5X concentrate" for flow cytometry. All other chemicals were purchased from Sigma/Aldrich, now

Millipore-Sigma (Burlington, MA). Hutner's trace elements were purchased from the University of Minnesota (Minneapolis, MN).

Equipment

Spectrophotometry was performed on a Molecular Dynamics (San Jose CA) M5e Spectrophotometer. Flow cytometry was performed on a Becton-Dickinson Accuri C + Plus flow cytometer (Franklin Lakes, NJ). Raman spectra were collected using a Renishaw inVia Raman Microscope coupled with Leica DM2500M microscope at the Dana-Farber Cancer Institute/Harvard Med. School, Boston, MA. A 785 nm diode laser was used for the surface enhanced Raman spectroscopy measurements.

Moonshot hardware was designed and built by The Bionetics Corporation, (Kennedy Space Center, Brevard County, FL) as an ultralow-power growth system for use on Artemis-1 [18]. Each of the three growth modules holds one standard 100 mm diameter circular Petri dish. The plates are illuminated with blue (~450 nm) and red (~660 nm) light-emitting diode (LED) lights continuously for 6 h in every 24 h. The combination of red and blue light is optimum for *Chlamydomonas* [50, 51]. The hardware monitors and records the temperature of the experiment, the power level, and draw from the batteries (as an indication that the lights were turned on and off), as well as the acceleration levels in three axes.

Once activated and loaded with the biological samples, the flight hardware was placed in a custom lathed form-fitting Styrofoam support and encased in a Nitex bag. The assembly was termed the BioExpt-01 Science Bag.

Crew Active Dosimeter (CAD) and Radiation Area Monitor (RAM) radiation detectors were placed adjacent to the biological flight hardware in the BioExpt-01 Science Bag. The detectors had been assembled and delivered to NASA/Kennedy Space Center prior to flight by the Space Radiation Analysis Group based at NASA Johnson Space Center (JSC) by Human Health and Performance Directorate/Leidos personnel. The detectors were collected post-flight and data was analyzed at NASA JSC [6].

Equipment

Spectrophotometry was performed on a Molecular Dynamics (San Jose CA) M5e Spectrophotometer. Flow cytometry was performed on a Becton-Dickinson Accuri C + Plus flow cytometer (Franklin Lakes, NJ). Raman spectra were collected using a Renishaw inVia Raman Microscope coupled with Leica DM2500M microscope at the Dana-Farber Cancer Institute/Harvard Med. School, Boston, MA. A 785 nm diode laser was used for the surface enhanced Raman spectroscopy measurements.

Moonshot hardware was designed and built by The Bionetics Corporation, (Kennedy Space Center, Brevard County, FL) as an ultralow-power growth system for use on Artemis-1 [18]. Each of the three growth modules holds one standard 100 mm diameter circular Petri dish. The plates are illuminated with

blue (~450 nm) and red (~660 nm) light-emitting diode (LED) lights continuously for 6 h in every 24 h. The combination of red and blue light is optimum for *Chlamydomonas* [50, 51]. The hardware monitors and records the temperature of the experiment, the power level, and draw from the batteries (as an indication that the lights were turned on and off), as well as the acceleration levels in three axes.

Once activated and loaded with the biological samples, the flight hardware was placed in a custom lathed form-fitting Styrofoam support and encased in a Nitex bag. The assembly was termed the BioExpt-01 Science Bag.

Crew Active Dosimeter (CAD) and Radiation Area Monitor (RAM) radiation detectors were placed adjacent to the biological flight hardware in the BioExpt-01 Science Bag. The detectors had been assembled and delivered to NASA/Kennedy Space Center prior to flight by the Space Radiation Analysis Group based at NASA Johnson Space Center (JSC) by Human Health and Performance Directorate/Leidos personnel. The detectors were collected post-flight and data was analyzed at NASA JSC [6].

Artemis-1 flight

After an initial delay of 19 days on the launch pad, the Artemis − 1 mission was launched from Kennedy Space Center (KSC) on November 16, 2022 for a planned 25-day space mission. Orion completed one flyby of the Moon on November 21, followed by a distant retrograde orbit for six days and then a second flyby of the Moon on November 25, and subsequently returned to Earth. The Orion capsule was recovered from the Pacific Ocean, returned to California, and transported back to KSC by truck. However, the Space Biology experiments were first removed from Orion in California, flown on an accompanied commercial flight to Kennedy Space Center at ambient temperature (without security radiation scanning) and the Moonshot hardware containing the samples, released to the investigators 9 days after the landing. The sample arrived back in the investigator's lab three days later, after decommissioning of the hardware at Bionetics facility adjacent to KSC. The samples for the payload described in the report were in the hardware for a total of 56.5 days (Fig. 1). The flight samples were exposed to microgravity in space, but also gravity transitions during launch and re-entry.

Analysis

Spectrophotometry

Chlamydomonas colonies were scraped from the agar, washed three times in phosphate buffered saline, resuspended in TAP buffer and assayed by spectrophotometry for chlorophyll a (absorbance at 436 nm), chlorophyll b (absorbance at 472 nm), photosystem I and II (absorbance at 700 nm and 680nm respectively but the peaks are too broad to separate), cytochrome f (absorbance at 554 nm), and protein

content (absorption at 800 nm). Net absorbance for each wavelength was calculated by subtracting the background absorbance of TAP buffer alone. The net absorbance values were then normalized to the protein content as measured by absorbance at 800 nm.

Flow Cytometry

Six colonies from flight and ground plates, plus four *Dsup* colonies from flight and ground plates, were harvested and resuspended in annexin-binding buffer, which is a phosphate buffer with calcium. The aggregates were disrupted by vortexing and then filtered through a 70µm nylon mesh to remove clumps that would plug the flow cytometer. The resuspended *Chlamydomonas* samples were aliquoted 100 µl per well into V-bottom microtiter plates. Individual aliquots were either stained with Alexa Fluor 488-annexin (5 µl/well) and propidium iodide (PI) (1 µl) to identify PCD and necrosis, or Nile Red (1:100 dilution from a stock solution of 100 µg ml^{-1} in methanol) with 0.005% Triton-X (1:100 dilution from a stock solution of 0.5% in water) permeabilization to measure lipid content.

We counted 2,000 *Chlamydomonas* cells from each sample. Background signal was estimated by appropriate no-dye controls. In every flow cytometry run, quality controls were performed on the instrument with three-color fluorescent beads, followed by assay of five control tubes: (1) no dyes, (2) Alexa fluor 488 annexin binding alone, (3) propidium iodide alone, (4) Alexa fluor 488 annexin binding with propidium iodide, and (5) Nile Red alone.

Flow cytometric and spectrophotometric data were evaluated by two-tailed Student's t-test comparing heat- or cold-exposed *Chlamydomonas* to the relevant room temperature control.

Single-cell confocal Raman spectroscopy of Chlamydomonas reinhardtii

Multiple colonies of *Chlamydomonas* were harvested from a ground plate, and flight plate. The samples included colonies flown live and colonies pretreated with azide before flight. The colonies were harvested into 1.5 ml Eppendorf tubes with 500 µL TAP and resuspended by pipetting and vortexing. The resultant *Chlamydomonas* solution was filtered through a 70 µm mesh into 12 x 74 mm polypropylene tubes to remove multicellular aggregates. The remaining solution of cells was divided into two 500 µL Eppendorf tubes, spun at 3000g for 1 minute to pellet the cells, and the supernatant aspirated. One tube was left to air dry. The second tube had 100 µL of 10% electron microscopy paraformaldehyde added, incubated for 10 min, and then was spun to pellet the cells before the supernatant was aspirated. This paraformaldehyde-fixed sample was washed with 500 µL deionized water, spun, and the supernatant aspirated.

A 2 µl aliquot of each sample rehydrated with distilled water was spotted on a quartz slide (25 mm x 25 mm x 1 mm) that was kept on a microscopic glass slide covered with aluminum foil. This substrate showed minimal background signal compared to various other substrates we tried such as glass, CaF_2 and Al_2O_3. A silicon wafer was not used as it has a strong Raman band at 521 cm^{-1} and interfered with

the current analysis. The samples were air dried at room temperature and were analyzed. A Horiba LabRAM Odyssey Raman microscope was used for the Raman spectral characterization of these samples. Laser power density was optimized in order to achieve better spectral intensity with characteristic Raman bands, which were not present at lower laser power densities. Exposure time and laser intensity were optimized by conducting a series of experiments to prevent charring of the samples to eliminate any unwanted signals due to laser-induced biomolecule denaturation. A 785 nm laser was used to acquire Raman spectra (acquisition time of 30 s with 300 lines/mm grating). First, white light focused on the individual algal cells at a magnification of 100X. Then, Raman spectra were collected in the range of 400–1800 cm^{-1}. The spectral baselines were pre-processed by polynomial fitting.

Statistics

Flow cytometric and spectrophotometric data are presented as geometric mean ± standard error with six replicates (unless otherwise noted). Correlations were analyzed by Statistica 6.1 (StatSoft Inc. Tulsa OK) using correlation matrix product moment and partial correlations.

For the Raman spectral analysis: Spectra were collected from five or more algal samples across three different colonies exposed to various conditions and subsequently averaged to better represent statistical variations in the intensities of vibrations corresponding to various biomolecular components within the spectra. The standard deviation of these intensities under different conditions was illustrated using error bars in the histogram to provide a clear visualization of the variability and reliability of our measurements.

Results

Moonshot hardware

The Moonshot hardware performed nominally throughout the flight and ground control experiments. The maximum temperature delta between flight and ground control hardware copies was 2.5^{o}F, well within the envelope of tolerable experimental conditions. At the end of the 25.5-day flight, the batteries still had more than 50% of power remaining. The power profile validated that the lights came on for 6 out of 24 h daily, as planned. Acceleration recordings show serial measurements of gravity in the z axis, but no acceleration in other directions as expected. The hardware met all the validation criteria for power use, power cycling, temperature control, g-force recording in three axes, data capture, and downloading for analysis, plus materials, and biological compatibility. The Moonshot hardware is now not only flight certified but flight proven.

Spectrophotometry of chlorophyll a and b, cytochrome f, and photosystem levels

Levels of the light absorbing pigments chlorophyll a and b, the mitochondrial heme protein cytochrome f, and the photon harvesting pigment photosystems were no different between ground and flight samples (Table 1).

Radiation exposure in assorted environments in space and on Earth

The total radiation exposure during the flight as measured in the RAM and CAD are reported in Table II. Comparison of the exposure levels during flight to other environmental systems (as shown in Table II) is examined in the discussion section.

Flow cytometry assay of viability and PCD of Chlamydomonas in Flight vs Ground

The percentages of PCD cells (Annexin V positive) and dead cells (propidium iodide positive) in the flight and ground control samples are shown in Fig. 2. 45.1 ± 1.4% of the cells in flight had undergone PCD compared to 31.1 ± 2.0% of the cells in the ground control (mean ± standard error, n = 6, $p < 0.001$). 53.9 ± 1.3% of the cells in flight were had undergone PCD, compared to 67.6 ± 1.9% of the cells in the ground control (mean ± standard error, n = 6, $p < 0.001$).

Flow cytometry assay of the effect of Dsup on the viability of Chlamydomonas in Flight vs Ground

The percentages of live cells (PI negative) in flown and ground control *Chlamydomonas* are shown in Fig. 3. 41.8 ± 1.7% of the flown cells with random gene inserts were living compared with 46.9 ± 2.3% of the flown cells with *Dsup* insertion (mean ± standard error, n = 6, $p < 0.001$). 16.4 ± 0.9% of the ground control cells with random gene inserts were living compared with 53.7 ± 2.6% of the ground control cells with *Dsup* insertion (mean ± standard error, n = 6, $p < 0.001$).

Single-cell confocal Raman spectroscopy of Chlamydomonas reinhardtii in Flight vs Ground

In this pioneering use of Raman spectroscopy for the analysis of space biology samples, we noticed a differential survival strategy among *Chlamydomonas* exposed to cosmic rays and/or microgravity. Specifically, we found two different cell types (Type I and Type II) with distinct Raman spectral features in flight samples compared to the ground samples. The intensity of Raman vibration corresponding to carotenoids in Type I cells (FL-Type I) was much weaker. Whereas, in Type II cells (FL-Type II), characteristic carotenoid vibrations were enhanced significantly (Fig. 4A). In Raman spectra of *Chlamydomonas*, the presence of prominent vibrations at 1001, 1156, and 1523 cm^{-1} indicate the presence of carotenoids [52–55], which are attributed to C–CH_3 deformation, C-C stretching, and C = C stretching vibrations of polyene, respectively [54, 56]. The significant variation in these carotenoid Raman vibrations found in the spectral profiles between Type I and Type II algal cells offers a compelling insight into the heterogeneity of stress responses within a single-cell population in two-cell populations. The lack of significant carotenoid vibrations in the Type I flight sample implies that these cells may not have been able to induce the same protective response and might have yielded to radiation-induced

damage. Moreover, the azide-killed flight samples exhibited nearly identical Raman spectra with weak carotenoid signal as in Type I cells, corroborating our proposed link between the absence of carotenoid and cell death pathways. The weaker carotenoid signals in these samples suggest that the living cells in the flight environment actively maintain or increase their carotenoid content. In contrast, the azide treatment or cell death ceases metabolic activity, thereby reducing the carotenoid levels.

For better understanding the relative increase in the carotenoid content at various conditions, the intensity ratio ($I_{Caro/Chlo}$) of carotenoid-chlorophyll vibration (1523 cm^{-1} and 1359 cm^{-1}, respectively) was used (Fig. 4C). We also used Raman spectroscopy to identify any significant changes in chlorophyll composition by analyzing prominent and characteristic Raman bands of chlorophylls found at 1359 (vibrations of C-C and C-N bonds within the porphyrin ring) and 1549 cm⁻1 (primarily involves the C = C stretching vibrations within the porphyrin ring) [57]. We noticed that the intensity ratio (Fig. 4B) of these bands ($I_{1549/1359}$) in flight samples (FL-Type I and FL-Type II) as well as in azide-killed samples, showed no significant differences compared to the ground sample, suggesting a comparable level chlorophyll levels across these conditions. This was in concordance with the data obtained from the spectrophotometry. A slight variation in the $I_{1549/1359}$ found in FL-Type II could potentially be due to the variation in chlorophyll a to chlorophyll b ratio as vibration corresponds to the stretching vibrations of the carbonyl (C = O) group in the aldehyde group present in Chlorophyll b also contributes to the intensity of Raman vibration at 1549 cm^{-1} (this ratio has slightly increased in FL-Type II samples). In addition, a minor shift in the 1549 cm^{-1} band to 1546 cm^{-1} in FL-Type II samples was also found, which could possibly be attributed to the change in the electronic environment around the chlorophyll molecules as an adaptive response to radiation stress and subsequent variation in chlorophyll b content.

Declarations

Author contributions

Author contributions were: Hardware design and build HWW, JMR, and TGH; Hands on biology experiments TGH, PLA, and HHB; Strain cloning HK, CN, and GG; Data management and statistics TGH and HHB; Administration services TGH, HLG, YZ, and HHB; Radiation dosimetry selection and management DD, and RG; Raman spectroscopy SP. Prose drafting TGH, SP, PD and HHB. All authors reviewed, edited, and approved multiple manuscript versions.

Competing interests

The authors declare no competing interests.

Author Contribution

Author contributions were: Hardware design and build HWW, JMR, and TGH; Hands on biology experiments TGH, PLA, and HHB; Strain cloning HK, CN, and GG; Data management and statistics TGH and HHB; Administration services TGH, HLG, YZ, and HHB; Radiation dosimetry selection and management DD, and RG; Raman spectroscopy SP. Prose drafting TGH, SP, PD and HHB. All authors reviewed, edited, and approved multiple manuscript versions.

Acknowledgement

This material is the result of work supported with resources and the use of facilities at the Durham Veterans Affairs Health Care System and Duke University School of Medicine. Contents do not represent the views of the Department of Veterans Affairs or the United States of America. CN and GG are both supported as Tier 1 Canadian Research Chairs.

Data Availability

All data is available in the NASA Research Repository. Contact Tim Hammond, the corresponding author, for information.

References

1. Bokharia, R. S. et al. Looking on the horizon; potential and unique approaches to developing radiation countermeasures for deep space travel. *Sci. Direct*. **35**, 105–112 (2022).
2. Torzillo, G., Scoma, A., Faraloni, C. & Giannelli, L. Advances in the biotechnology of hydrogen production with the microalga Chlamydomonas reinhardtii. *Crit. Rev. Biotechnol.* **35** (4), 485–496 (2015).
3. Scaife, M. A. et al. Establishing Chlamydomonas reinhardtii as an industrial biotechnology host. *Plant. J.* **82** (3), 532–546 (2015).
4. Simonsen, L. C., Slaba, T. C., Guida, P. & Rusek, A. NASA's first ground-based galactic cosmic ray simulator: Enabling a new era in space radiobiology research. *PLoS Biol.* **18**, e3000669. 10.1371/journal.pbio.3000669 (2020).
5. Kodaira, S. et al. Space radiation dosimetry at the exposure facility of the International Space Station for the Tanpopo mission. *Astrobiology*. **21** (12), 1473–1478 (2021).
6. Gaza, R. et al. The importance of time-resolved personal dosimetry in space: The ISS crew active dosimeter. *Life sciences in space research*. 39, pp. 95–105 (2023).
7. Bertalan, I., Esposito, D. & Torzillo, G. Photosystem II stress tolerance in the unicellular green alga Chlamydomonas Reinhardtii under space conditions. *Microgravity Sci. Technol.* **19**, 122–127 (2007).
8. Durand, P. M., Choudhury, R., Rashidi, A. & Michod, R. E. Programmed death in a unicellular organism has species-specific fitness effects. *Biol. Lett.* **10**, 20131088. 10.1098/rsbl.2013.1088 (2014).

9. Zeballos, N., Grulois, D., Leung, C. & Chevin, L. M. Acceptable loss: Fitness consequences of salinity-induced cell death in a halotolerant microalga. *Am. Nat.* **201** (6), 825–840 (2023).
10. Barreto Filho, M. M., Bagatini, I. L. & Durand, P. M. How shall we measure programmed cell death in eukaryotic microalgae? *Eur. J. Phycol.* **58** (1), 13–34 (2022).
11. Panikkanvalappil, S. R., Hira, S. M., Mahmoud, M. A. & El-Sayed, M. A. Unraveling the biomolecular snapshots of mitosis in healthy and cancer cells using plasmonically-enhanced Raman spectroscopy. *J. Am. Chem. Soc.* **136** (45), 15961–15968 (2014).
12. Panikkanvalappil, S. R., Hira, S. M. & El-Sayed, M. A. Elucidation of ultraviolet radiation-induced cell responses and intracellular biomolecular dynamics in mammalian cells using surface-enhanced Raman spectroscopy. *Chem. Sci.* **7** (2), 1133–1141 (2016).
13. Sharma, S. et al. Diverse organic-mineral associations in Jezero crater. *Mars Nat.* **619**, 724–732 (2023).
14. Panikkanvalappil, S. R., Hira, S. M. & El-Sayed, M. A. Elucidation of ultraviolet radiation-induced cell responses and intracellular biomolecular dynamics in mammalian cells using surface-enhanced Raman spectroscopy. *Chem. Sci.* **7** (2), 1133–1141 (2016).
15. Panikkanvalappil, S. R. et al. Hyperoxia Induces Intracellular Acidification in Neonatal Mouse Lung Fibroblasts: Real-Time Investigation Using Plasmonically Enhanced Raman Spectroscopy. *J. Am. Chem. Soc.* **138** (11), 3779–3788 (2016).
16. Puig, J., Knodlseder, N., Quera, J., Algara, M. & Guell, M. DNA damage protection for enhanced bacterial survival under simulated low Earth orbit environmental eonditions in *Escherichia coli*. *Front. Microbiol.* **12**, 789668 (2021).
17. Hashimoto, T. & Kunieda, T. DNA protection protein, a novel mechanism of radiation tolerance: lessons from tardigrades. *Life (Basel)*. **7**, 26. 10.3390/life7020026 (2017).
18. Hammond, T. G. et al. Moonshot: Affordable, simple, flight hardware for the Artemis-1 mission and beyond. *Front. Space Technol.* **1**, 593523. 10.3389/frspt.2020.593523 (2020).
19. Prasad, B. et al. Influence of microgravity on apoptosis in cells, tissues, and other systems in vivo and in vitro. *Int. J. Mol. Sci.* **21**, 9373. 10.3390/ijms21249373 (2020).
20. Papadopoulos, A. et al. Space radiation quality factor for galactic cosmic rays and typical space mission scenarios using a microdosimetric approach. *Radiat. Environ. Biophys.* **62** (2), 221–234 (2023).
21. Mehner, C. et al. Real versus simulated galactic cosmic radiation for investigating cancer risk in the hematopoietic system - are we comparing apples to apples? *Life sciences in space research*. 29, pp. 8–14 (2021).
22. Sishc, B. J. et al. The need for biological countermeasures to mitigate the risk of space radiation-Induced carcinogenesis, cardiovascular disease, and central nervous system deficiencies. *Life Sci. space Res.* **35**, 4–8 (2022).
23. Kojic, M. & Milisavljevic, M. When disaster strikes: Reconstitution of population density by expansion of survivors. *Mol. Ecol.* **29** (24), 4757–4764 (2020).

24. Durand, P. M. & Ramsey, G. The concepts and origins of cell mortality. *History and Philosophy of the Life Sciences* 45, 23 DOI: (2023). https://doi.org/10.1007/s40656-023-00581-8
25. Barreto Filho, M. M., Vieira, H. H., Morris, J. J. & Bagatini, I. L. Species-specific effects and the ecological role of programmed cell death in the microalgae *Ankistrodesmus* (Sphaeropleales, Selenastraceae). *Biol. Lett.* **18**, 20220259. 10.1098/rsbl.2022.0259 (2022).
26. Durand, P. M. Mechanisms and Measures of Programmed cell Death in the Unicellular World, in The Evolutionary Origins of Life and Death, University of Chicago Press. 89–1056. (2021).
27. Ding, M. & Baker, D. Recent advances in high-throughput flow cytometry for drug discovery. *Expert Opin. Drug Discov*. **16** (3), 303–317 (2021).
28. Goldstein, B. & Blaxter, M. *Tardigrades Curr. biology: CB* **12**(14), R475 (2002).
29. Horikawa, D. D. et al. Radiation tolerance in the tardigrade Milnesium tardigradum. *Int. J. Radiat. Biol.* **82** (12), 843–848 (2006).
30. Jonsson, K. I., Harms-Ringdahl, M. & Torudd, J. Radiation tolerance in the eutardigrade Richtersius coronifer. *Int. J. Radiat. Biol.* **81** (9), 649–656 (2005).
31. Jonsson, K. I., Rabbow, E., Schill, R. O., Harms-Ringdahl, M. & Rettberg, P. Tardigrades survive exposure to space in low Earth orbit. *Curr. biology: CB*. **18** (17), R729–R731 (2008).
32. Kasianchuk, N., Rzymski, P. & Kaczmarek, L. The biomedical potential of tardigrade proteins: A review. *Biomed. Pharmacother*. **158**, 114063. 10.1016/j.biopha.2022.114063 (2023).
33. Jonsson, K. I. Tardigrades as a potential model organism in space research. *Astrobiology*. **7** (5), 757–766 (2007).
34. Weronika, E. & Lukasz, K. Tardigrades in space research - past and future. *Orig Life Evol. Biosph*. **47** (4), 545–553 (2017).
35. Kamal, K. Y. & Lawler, J. M. Cellular and molecular signaling meet the space environment. *Int. J. Mol. Sci.* **24**, 5955. 10.3390/ijms24065955 (2023).
36. Pohjoismaki, J. L. O. & Goffart, S. Adaptive and pathological outcomes of radiation stress-induced redox signaling. *Antioxid. Redox. Signal.* **37** (4–6), 336–348 (2022).
37. Farhood, B. et al. Targeting of cellular redox metabolism for mitigation of radiation injury. *Life Sci.* **250**, 117570. 10.1016/j.lfs.2020.117570 (2020).
38. Caferri, R., Guardini, Z., Bassi, R. & Dall'Osto, L. Chapter Two - Assessing photoprotective functions of carotenoids in photosynthetic systems of plants and green algae, in *Methods in Enzymology*, E.T. Wurtzel, Editor, Academic Press. pp. 53–84. (2022).
39. Bast, A., van der Plas, R. M., van den Berg, H. & Haenen, G. R. Beta-carotene as antioxidant. *Eur. J. Clin. Nutr.* **50**, S54–56 (1996).
40. Patrick, L. Beta-carotene: the controversy continues. *Altern. Med. Rev.* **5** (6), 530–545 (2000).
41. Sankari, M., Hridya, H., Sneha, P., George Priya Doss, C. & Ramamoorthy, S. Effect of UV radiation and its implications on carotenoid pathway in Bixa orellana L. *J. Photochem. Photobiol B*. **176**, 136–144. 10.1016/j.jphotobiol.2017.10.002 (2017).

42. Saini, R. K. & Keum, Y. S. Significance of Genetic, Environmental, and Pre- and Postharvest Factors Affecting Carotenoid Contents in Crops: A Review. *J. Agric. Food Chem.* **66** (21), 5310–5324 (2018).
43. Stoffle, N. N. et al. HERA: A Timepix-based radiation detection system for Exploration-class space missions. *Life sciences in space research*. 39, pp. 59–66 (2023).
44. Berger, T. et al. The German Aerospace Center M-42 radiation detector-A new development for applications in mixed radiation fields. *Rev. Sci. Instrum.* **90**, 125115. 10.1063/1.5122301 (2019).
45. Zeitlin, C. et al. Measurements of energetic particle radiation in transit to Mars on the Mars Science Laboratory. *Science*. **340** (6136), 1080–1084 (2013).
46. Ruhm, W. et al. Typical doses and dose rates in studies pertinent to radiation risk inference at low doses and low dose rates. *J. Radiat. Res.* **59** (suppl_2), ii1–ii10 (2018).
47. *Radiation Dose from X-rays and CT Exams* https://www.radiologyinfo.org/en/info/safety-xray
48. George, S. P. et al. Space radiation measurements during the Artemis I lunar mission. *Nature*. **634** (8032), 48–52 (2024).
49. Hammond, T. G. & Hammond, J. M. Optimized suspension culture: the rotating-wall vessel. *Am. J. Physiol. Ren. Physiol.* **281** (1), F12–25 (2001).
50. Oldenhof, H., Zachleder, V. & Van Den Ende, H. Blue- and red-light regulation of the cell cycle in *Chlamydomonas reinhardtii* (Chlorophyta). *J. Phycol.* **41** (3), 313–320 (2006).
51. Li, X. et al. An Indexed, Mapped Mutant Library Enables Reverse Genetics Studies of Biological Processes in Chlamydomonas reinhardtii. *Plant. Cell.* **28** (2), 367–387 (2016).
52. Jehlička, J. et al. Potential and limits of Raman spectroscopy for carotenoid detection in microorganisms: implications for astrobiology. *Philosophical Transactions of the Royal Society A: Mathematical, Physical and Engineering Sciences*. 372 p. 20140199 (2014). (2030).
53. Udensi, J., Loughman, J., Loskutova, E. & Byrne, H. J. Raman Spectroscopy of Carotenoid Compounds for Clinical Applications—A Review. *Molecules*. **27** 10.3390/molecules27249017 (2022).
54. de Oliveira, V. E., Castro, H. V., Edwards, H. G. M. & de Oliveira, L. F. C. Carotenes and carotenoids in natural biological samples: a Raman spectroscopic analysis. *J. Raman Spectrosc.* **41** (6), 642–650 (2010).
55. Udensi, J., Loughman, J., Loskutova, E. & Byrne, H. J. Raman spectroscopy of carotenoid compounds for clinical applications-A review. *Molecules*. **27**, 9017. 10.3390/molecules27249017 (2022).
56. Vítek, P., Osterrothová, K. & Jehlička, J. Beta-carotene—A possible biomarker in the Martian evaporitic environment: Raman micro-spectroscopic study. *Planet. Space Sci.* **57** (4), 454–459 (2009).
57. Cai, Z. L., Zeng, H., Chen, M. & Larkum, A. W. D. Raman spectroscopy of chlorophyll d from Acaryochloris marina. *Biochim. et Biophys. Acta (BBA) - Bioenergetics*. **1556** (2), 89–91 (2002).

58. Hassler, D. M. et al. Mars' surface radiation environment measured with the Mars Science Laboratory's Curiosity rover. *Science*. **343**, 1244797. 10.1126/science.1244797 (2014).

Tables

Table 1
Relative quantities of protein in flown vs. ground control *Chlamydomonas*

Protein (OD 800)	Flight Avg	Flight SEM	Ground Avg	Ground SEM	T-test
Chlorophyll a (OD 436)	1.244	0.049	1.257	0.038	NS
Chlorophyll b (OD 472)	1.273	0.044	1.266	0.030	NS
Cytochrome f (OD 554)	1.111	0.027	1.119	0.014	NS
Photosystem I and II (OD 700)	1.153	0.017	1.141	0.014	NS

Table 1. Aliquots of flown and ground control *Chlamydomonas* were suspended in TAP and the optical densities (ODs) for chlorophyll a (OD 436), chlorophyll b (OD 472), cytochrome f (OD 554) and photosystem I and II (OD 700) were measured by spectrophotometry. Values shown are the net OD above background absorbance for TAP media alone, normalized to the total quantity of protein measured as OD 800. Values are the mean and SEM of six replicates. Significance was estimated by unpaired t-test, with non-significant differences (NS) defined as $p>0.05$.

Table II Radiation exposure in assorted environments in space and on Earth

Exposure	Radiation (mGy)	Ref.
Radiation Area Monitor Artemis I Mission Dose	11.4 ± 0.4	[6]
Crew Active Dosimeter Artemis I Mission Dose	12.6 ± 0.5	[6]
Naturally occurring "background" for 25.5 days (Earth)	0.17	[46]
CAT-Scan of Abdomen & Pelvis, ± contrast	15.4	[47]
Exposure on Mars for 25.5 days (Curiosity rover)	5.4	[45, 58]
Mars transit for 25.5 days (Curiosity rover)	11.8	[45, 58]
International Space Station for 25.5 days	5.7	[5]

Table II. Comparison of total radiation doses for 25.5 days during the Artemis I mission, plus 25.5 days of exposure to background radiation on Earth, the Curiosity rover in transit to Mars, and on Mars, and 25.5 days on the ISS. CAT-scan exposure is a one-time dose.

Figures

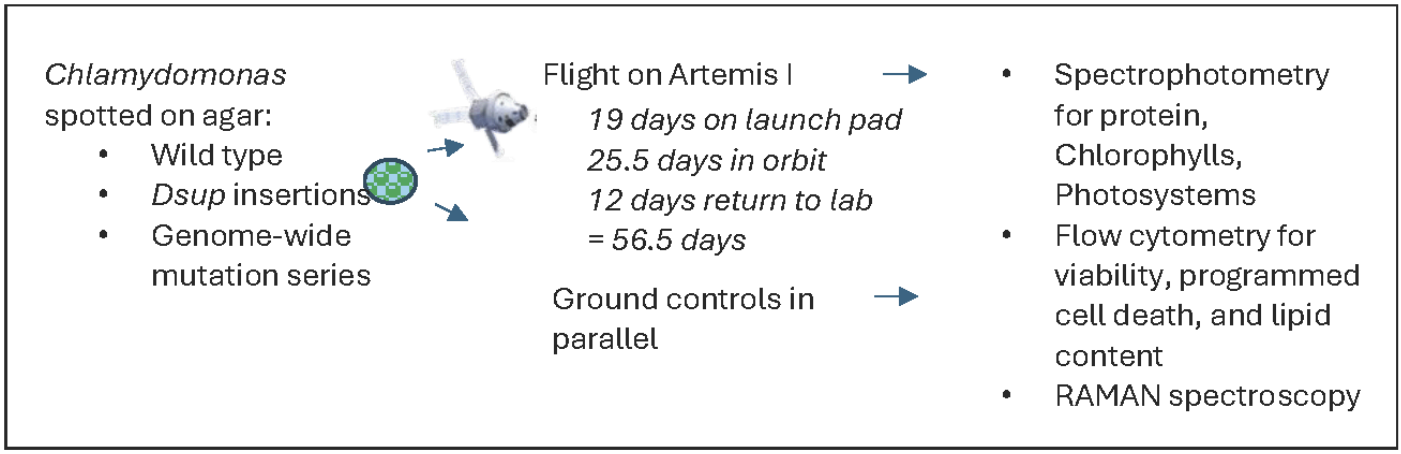


Figure 1

Schematic of experiments. A summary diagram of *Chlamydomonas* preparation, flight details, and analysis modalities.

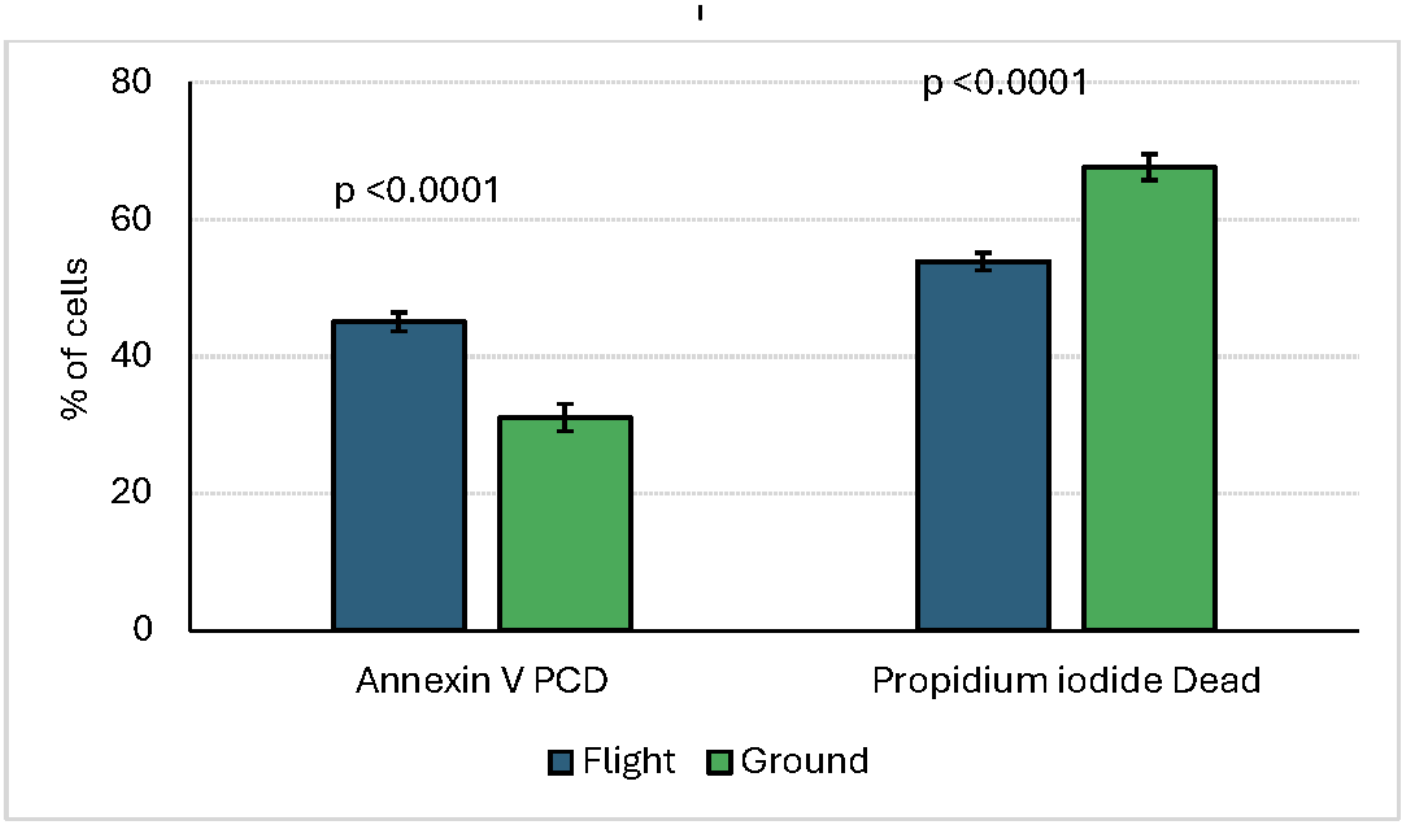


Figure 2

Viability and programmed cell death (PCD) of *Chlamydomonas* in Flight vs Ground. Aliquots of flown and ground control *Chlamydomonas* were stained with Annexin V, to identify PCD, and propidium iodide, to identify dead cells, and analyzed by flow cytometry. Values shown are the % positively staining cells and are the mean ± SEM of six replicates. The p values for significance were evaluated by unpaired two-tailed t-test.

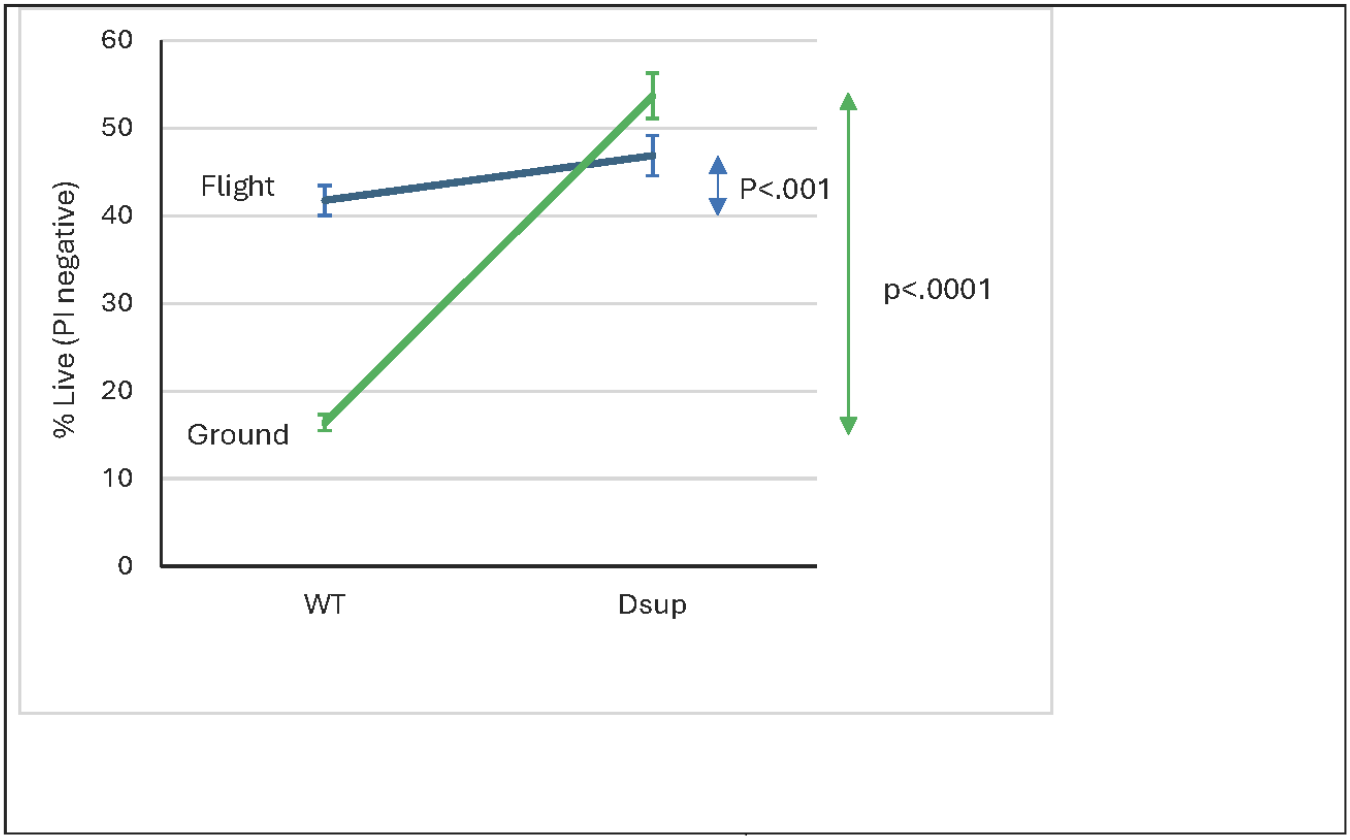


Figure 3

Effect of *Dsup* on the viability of *Chlamydomonas* in Flight vs Ground. *Chlamydomonas* with insertion of the *Dsup* gene were compared to wild type (WT) strains in flown versus ground control samples. Aliquots of each were stained with propidium iodide and analyzed by flow cytometry. Values shown are the percent of viable cells, defined as excluding propidium iodide, and are the mean ± SEM of six replicates. The p values for significance were evaluated by unpaired two-tailed t-test.

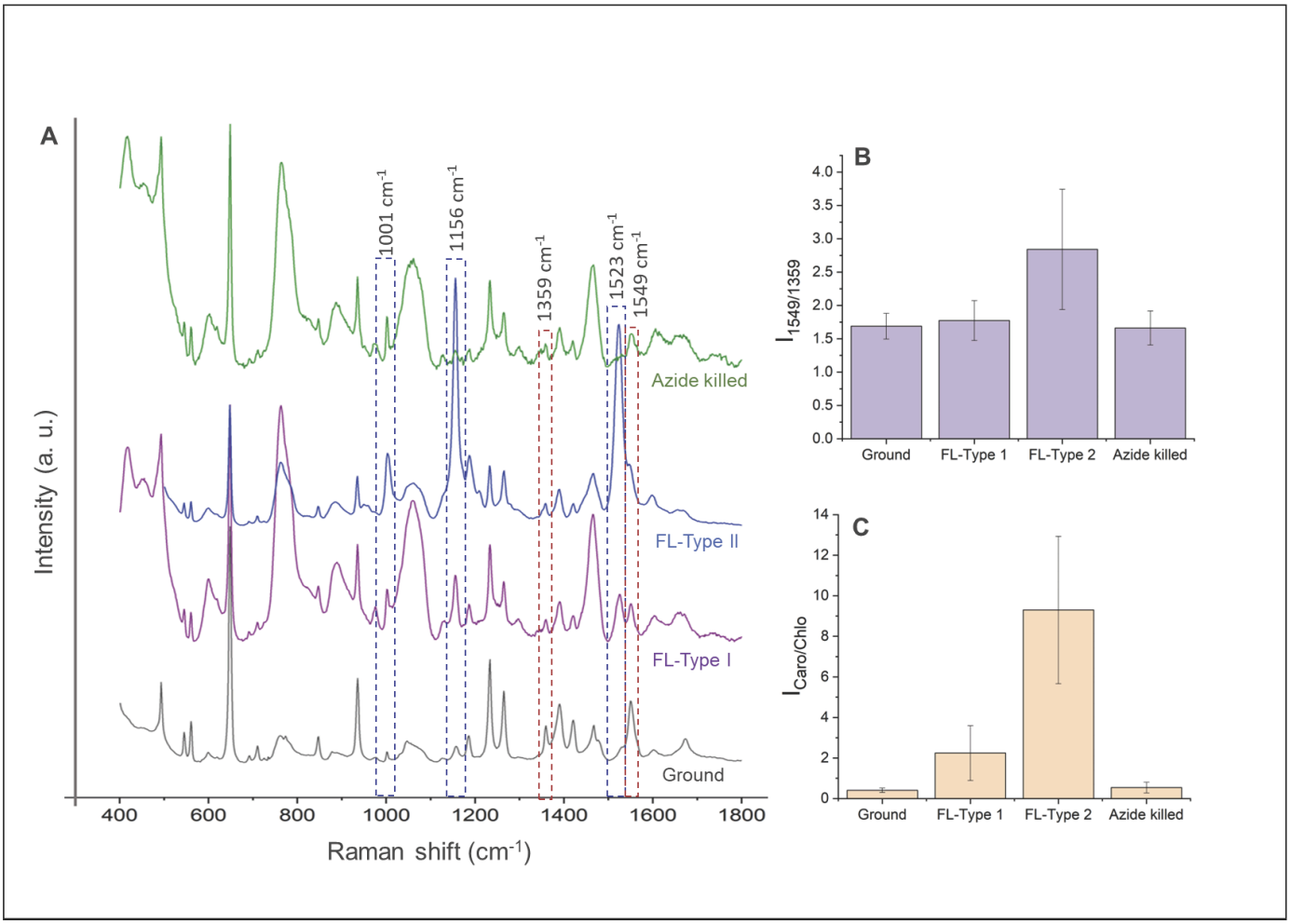


Figure 4

Raman spectra from ground control *Chlamydomonas* and Type I, Type II, and azide-killed cells from flown *Chlamydomonas*.

Raman spectra of *Chlamydomonas* under different conditions are shown in **Fig 4A**. Prominent Raman shifts at 1001, 1156, 1359, 1523, and 1549 cm^{-1}, associated with various molecular vibrations, are highlighted with dashed boxes. Histograms showing the ratio of the intensities of the Raman bands at 1549 cm^{-1} and 1359 cm^{-1} ($I_{1549/1359}$) for various samples are shown in **Fig 4B**. Flown *Chlamydomonas* contained two different cell types (Type I and Type II) with distinct Raman spectral features. The intensity of Raman vibration corresponding to carotenoids in Type I cells (FL-Type I) was much weaker. Whereas, in Type II cells (FL-Type II), characteristic carotenoid vibrations enhanced significantly. This ratio provides the relative chlorophyll content across different conditions. Histogram illustrating the carotenoid to chlorophyll ratio ($I_{Caro/Chlo}$) across the various sample types are shown in **Fig 4C**. The data points represent the mean value and error bars indicate the standard deviation, reflecting the variability of the response in each sample type. These spectra and ratios provide insights into the biochemical

adaptations of *Chlamydomonas* to galactic radiation and microgravity, with significant variations noted between the two cell types we found in live flight samples, suggesting differential stress responses and survival strategies.